Invert Neurosci (2006) 6: 57–68
DOI 10.1007/s10158-006-0018-y

ORIGINAL PAPER

Irina Vinogradova · Alan Cook · Lindy Holden-Dye

The ionic dependence of voltage-activated inward currents in the pharyngeal muscle of *Caenorhabditis elegans*

Received: 27 February 2006 / Accepted: 22 March 2006 / Published online: 19 April 2006

Abstract The pharynx of *Caenorhabditis elegans* consists of a syncytium of radially orientated muscle cells that contract synchronously and rhythmically to ingest and crush bacteria and pump them into the intestine of the animal. The action potentials that support this activity are superficially similar to vertebrate cardiac action potentials in appearance with a long, calcium-dependent plateau phase. Although the pharyngeal muscle can generate action potentials in the absence of external calcium ions, action potentials are absent when sodium is removed from the extracellular solution (Franks et al. 2002). Here we have used whole cell patch clamp recordings from the pharynx and show low voltage-activated inward currents that are present in zero external calcium and reduced in zero external sodium ions. Whilst the lack of effect of zero calcium when sodium ions are present is not surprising in view of the known permeability of voltage-gated calcium channels to sodium ions, the reduction in current in zero sodium when calcium ions are present is harder to explain in terms of a conventional voltage-gated calcium channel. Inward currents were also recorded from *egl-19* (*n582*) which has a loss of function mutation in the pharyngeal L-type calcium channel and these were also markedly reduced in zero external sodium. Despite this apparent dependence on external sodium ions, the current was partially blocked by the divalent cations, cadmium, barium and nickel. Using single-channel recordings we identified a cation channel for which the open-time duration was increased by depolarisation. In inside-out patches, the single-channel conductance was highest in symmetrical sodium solution. Further studies are required to determine the contribution of these channels to the pharyngeal action potential.

I. Vinogradova · A. Cook · L. Holden-Dye (✉)
Neurosciences Research Group, School of Biological Sciences,
Bassett Crescent East, University of Southampton,
Southampton SO16 7PX, UK
E-mail: lmhd@soton.ac.uk
Tel.: +44-2380-594295
Fax: +44-2380-594459

Keywords *C. elegans* · Pharynx · Sodium current · Calcium current · Single-channel recording

Introduction

Caenorhabditis elegans is a microscopic free-living nematode with a fully sequenced genome. This has provided an opportunity to predict the entire complement of ion channels in a single animal. For example, it has been shown that *C. elegans* express a number of voltage-gated calcium (Goodman et al. 1998; Lee et al. 1997; Richmond and Jorgensen 1999) and potassium channels (Wei and Salkoff 1996; Richmond and Jorgensen 1999) as well as amiloride-sensitive sodium channels (O'Hagan et al. 2005) and different types of ligand-gated ion channels (Jorgensen and Nonet 1995; Hart et al. 1995; Maricq et al. 1995; Li et al. 1997; see Bargmann 1998 for review). One of the most intriguing features of this animal's genome is that homology searches reveal no evidence for voltage-gated sodium channels (Bargmann 1998). Their absence is surprising as these channels play a critical role in determining the excitability of nerve and muscle cells for the vast majority of animals from different phyla. In recent patch-clamp experiments on *C. elegans* neurones (Goodman et al. 1998) and body wall muscle cells (Richmond and Jorgensen 1999; Jospin et al. 2002) no sodium currents were observed. However, intracellular recordings from pharyngeal muscle cells have shown a dependence of spike generation on external sodium (Franks et al. 2002). Although neither spiking frequency, nor the waveform of pharyngeal action potentials, were sensitive to tetrodotoxin and saxitoxin, the action potentials were blocked by procaine and quinidine (Franks et al. 2002), which are also known to block sodium channels. Furthermore, the frequency of action potentials was potentiated by veratridine, a toxin which shifts the voltage-dependence of activation of sodium channels and slows down the rate of inactivation (Ulbricht 1969; Ohta et al. 1973; Barnes and Hille 1988).

There are a number of possible explanations for the effect of zero external sodium ions on pharyngeal action potentials. For example, this property could derive from a sodium-dependent, neurogenic pacemaker event. There is evidence that the cholinergic motorneurone MC acts a pharyngeal pacemaker neurone (Raizen et al. 1995) and this involves a nicotinic acetylcholine receptor subunit EAT-2 (McKay et al. 2004). Whilst it would be predicted that the nicotinic channel is a non-selective cation channel, and therefore would not be selectively affected by a reduction in external sodium ion concentration, nonetheless, the possibility that removal of external sodium ions affects this pacemaker activity cannot be discounted. Alternatively, the pharyngeal muscle may have some myogenic activity (Avery and Horvitz 1989). The mechanism for this is not understood, but if it requires sodium ions then this may also provide an explanation for the sodium-dependence of the pharyngeal action potentials. Thirdly, it is possible that this sodium-dependence derives from the ionic selectivity of voltage-gated ion channels that contribute to the pharyngeal action potential. This study addresses this latter possibility by making whole cell and single-channel recordings from the pharynx.

Methods

Caenorhabditis elegans (N2 Bristol strain) were cultured on agar and fed with *E. coli* (OP50 strain). Adult hermaphrodite animals were picked from 3- to 5-day-old plates. The worms were placed in Dent's solution of the following composition (in mM): 140 NaCl, 6 KCl, 10 glucose, 5 HEPES, 3 $CaCl_2$, 1 $MgCl_2$, pH 7.4, and transiently cooled to immobilize them. The anterior region was sectioned from the rest of the body at the level of the pharyngeal intestinal valve and transferred to a custom-built perfusion chamber (volume 2.5 ml) on a glass coverslip. The recording chamber was mounted on an Olympus inverted microscope.

For each experiment a dissected anterior region was fixed in the experimental chamber with the help of a suction electrode leaving the terminal bulb free. The preparation was consecutively treated (protocol modified from Richmond and Jorgensen 1999) with 1 mg/ml trypsin (30–50 s) and a mixture of 0.23 mg/ml protease type IV and 0.63 mg/ml collagenase P for 1–4 min. After the completion of the enzymatic treatment the preparation was perfused via gravity feed with Dent's saline at a rate of 5 ml/min. All drugs were applied by addition to the perfusate.

Patch electrodes for whole-cell recordings were pulled from Haematokrit capillaries (resistance 3–5 MΩ, filled with internal solutions of the following composition, in mM: 150 *N*-methyl-D-glucamine, 4 $MgCl_2$, 5 HEPES, 0.25 $CaCl_2$, 36 sucrose, 5 EGTA or 140 CsCl, 5 HEPES, 5 TEA, 0.3 $CaCl_2$, 5 CsBAPTA, pH 7.2). Whole-cell recordings were achieved in a conventional manner, by making gigaohm seals and breaking through the membrane by suction. The inward currents recorded with either of these solutions were similar. (The solution used for individual experiments is noted in the figure legends.) The reference electrode was a silver chloride coated silver pellet connected directly to the recording chamber. The measured junction potential under these conditions was 2.5 mV and was not corrected for.

In ion replacement experiments, sodium chloride was replaced with either sodium isethionate or *N*-methyl-D-glucamine.

To check for intercellular coupling (Starich et al. 1996) between muscle cells in the terminal bulb 0.5% 5,6 carboxyfluorescein was added to the intracellular solution. For comparison, and to visualize individual cells, the gap junction impermeable marker tetramethylrhodamine dextran was used at a concentration 0.5% in the intracellular solution.

Single-channel recordings were performed in outside-out and inside-out configuration using thick-walled electrodes (GC150-7.5 glass, Harvard Apparatus). The electrode tips were coated with beeswax and fire polished. For channel recording in outside-out configuration pipettes were filled with caesium containing internal solution as stated above. In some experiments chloride was exchanged for aspartate in the internal solution. Composition of the caesium aspartate internal solution was (in mM): 130 CsOH; 5 BAPTA; 100 D-aspartic acid; 10 MOPS; 5 TEA; 10 NaCl, pH 7.2. In experiments with inside-out patches symmetrical sodium and calcium solutions were used. The composition of symmetrical sodium solution was (in mM): 150 NaCl; 5 TEA; 5 HEPES; 2 $MgCl_2$. To test the effect of calcium ions on the external side of the membrane 3 mM $CaCl_2$ was added to this solution and used as pipette solution. The composition of the symmetrical calcium solution was (in mM): 140 NmDG; 5 $CaCl_2$; 5 TEA; 5 HEPES; 2 $MgCl_2$. Resistance of electrodes used for single-channel recordings was 8–10 MΩ.

Data were acquired with an Axopatch1D amplifier at the bandwidth of 5 kHz for whole-cell, and 1–2 kHz for single-channel recordings, digitised at 10 kHz using Pclamp7 software and stored on a hard disk for off-line analysis. After seal formation (seal resistance in the range of 10–30 GΩ) whole cell currents were recorded during 150 ms steps, with 10 mV increments from the holding potentials. Leak subtraction was performed using the P/4 protocol. In experiments where cell capacitance transients were recorded (without leak subtraction) in response to 2 mV steps from a holding potential (V_h) of −80 mV the data were used to calculate whole-cell capacitance after integrating the area under the curve in Clampfit8 (Axon Instruments). Due to electrical coupling between pharyngeal muscle cells (see Results), only partial whole-cell capacitance compensation was possible.

Single-channel activity was recorded from outside-out patches at V_h of −80, −40, 0 and +40 mV, or during 400 ms steps with 10 mV increment from V_h −80 mV after a 50 ms prepulse to −100 mV.

No leak subtraction was performed during acquisition of single-channel activity.

Amplitudes and open-time duration of unitary events were measured using Fetchan pClamp software, and analysed with pStat. Distributions of current amplitudes and open times were obtained for each individual outside-out patch. Open-time distributions were fitted by a single exponential and the time-constant, tau (τ), of the distribution curve was determined in order to characterise the potential-dependence of the open time (Horn and Vandenberg 1984).

NP_o (where N is the number of channels in a patch and Po is the probability of opening) at V_h −80 mV was calculated by adding the time duration of all openings and dividing the sum by the duration of the analysed time interval. During steps to −30 mV from V_h −100 mV (200 steps were analysed for each patch) NP_o was evaluated sweep by sweep; null traces were included in the calculation of mean NP_o. Chord conductance g_{Na}, was calculated from the equation $I_{Na} = g_{Na}(V - E_{Na})$, assuming $E_{Na} = +66$ mV in Dent's solution.

All chemicals were purchased from Sigma (Poole, UK). Collagenase P was purchased from Boehringer–Mannheim (London, UK) and tetramethylrhodamine dextran from Molecular Probes (Paisley, UK).

Data are presented as the mean ± standard error of the mean. The amplitude of whole cell currents was measured as the peak amplitude within 50 ms of the voltage step. As it was not technically possible to completely compensate for capacitance, currents are expressed as pA and have not been normalised for expression as pA/pF. The effects of ionic substitution and channel blockers have been expressed as a percentage of the control current, where 'control' is the current recorded from the same cell immediately prior to application of the test solution. Statistical significance was analysed using the Student's paired *t* test, applied to non-normalised data sets, with a significance level of $P < 0.05$.

The mutants *eat-5* (*ad464*) strain DA464, and *egl-19* (*n582*) strain MT1212, were obtained from the *Caenorhabditis* Genetics Center.

Results

Whole-cell recordings

The whole-cell capacitance estimated by integration of the area under capacitance transients was very high (443 ± 54 pF, $n = 21$) and could not be completely compensated. Although the surface area of the pharyngeal muscle has many folds which will contribute to this high capacitance, a major factor is likely to be electrical coupling between muscle cells through gap junctions (Starich et al. 1996). When the whole-cell configuration was obtained using patch pipettes filled with solution containing carboxyfluorescein the whole terminal bulb as well as isthmus became intensely fluorescent (Fig. 1a) consistent with a strong coupling between pharyngeal cells. The coupling may be stronger than that described by Starich et al. (1996) due to the lower intracellular calcium concentration in cells internally perfused with EGTA. In order to improve the conditions for whole-cell voltage clamp, we attempted to uncouple cells using the gap junction blocker, carbenoxolone (120–240 μM), but without success. We also tested whether *eat-5* mutants, with impaired gap junctions (Starich et al. 1996), may have less dye-coupling between pharyngeal muscle cells and therefore potentially be more amenable to voltage-clamp. However, we also observed dye-coupling in *eat-5* (data not shown). We concluded that it was not possible to minimise electrical coupling between cells to improve the conditions for voltage-clamp analysis. However, addition of the gap junction impermeant fluorescent marker, tetramethylrhodamine dextran, to the intracellular solution allowed identification of the muscle cell in the terminal bulb from which recordings were made (Fig. 1b).

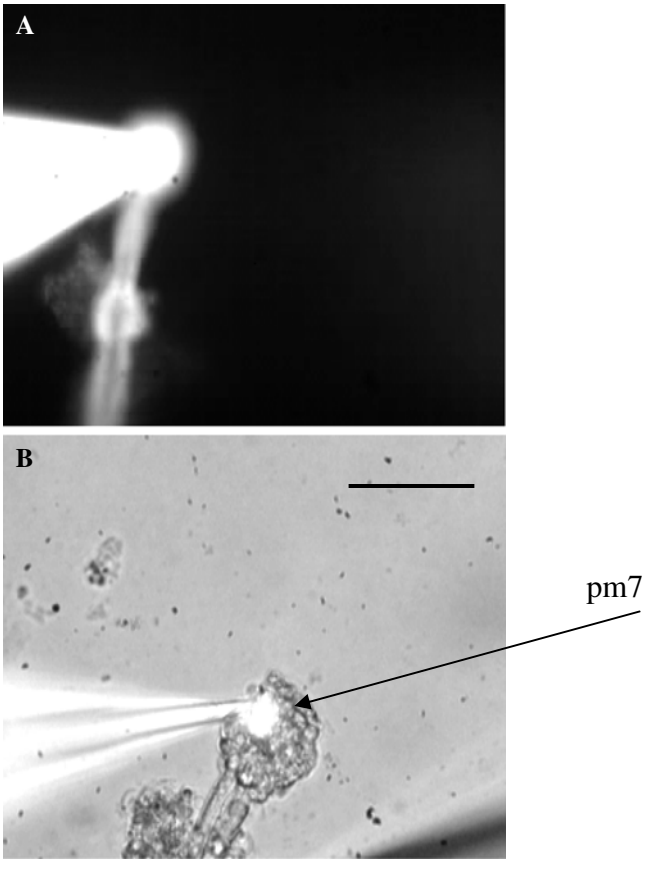

Fig. 1 Images of the pharyngeal preparation after establishing whole-cell recording. **a** The recording pipette (on the *left*) contains carboxyfluorescein which has diffused into the pharyngeal muscle cells and labelled the entire pharynx by permeating gap junctions. **b** An overlay of a bright field and fluorescence image. The recording pipette (on the *left*) contains tetra-rhodamine dextran which does not permeate gap junctions. A single muscle cell, pm7 is labelled with fluorescence. Scale bar (**a**, **b**) 10 μm

Limitations of the pharyngeal preparation for measuring voltage-activated inward currents

Voltage-activated currents were recorded from the terminal bulb of the pharyngeal muscle. The mono-exponential decay of the whole-cell capacitance transients, together with the absence of spike generation during depolarising steps suggests reasonably good voltage control over the small terminal bulb (diameter less than 10 μM). However, the extensive electrical coupling between the muscle cells indicates that the voltage-activated currents, particularly the long-latency currents observed during larger depolarising steps, are unlikely to be recorded from an area of uniform potential. Indeed, the observation of 'notches' of inward current, of varying degrees of severity, during the later stage of the voltage-steps (Fig. 2a) indicates that the currents are not recorded from a region at isopotential. (Fig. 2b shows an extreme example of this.) Furthermore, we were unable to generate current–voltage plots that showed a reversal for these inward currents (Fig. 2c), further supporting the contention that the pharynx is not accurately clamped during large depolarising steps. These factors placed limitations on the analysis of the kinetics and voltage-dependence of the inward currents and therefore we restricted our investigation to the ionic dependence of the short latency current that peaks within 50 ms of the depolarising voltage step. The majority of this current would be predicted to arise from channels in the immediate vicinity of the electrode i.e. in the muscle cell of the terminal bulb, where the membrane voltage is most accurately clamped.

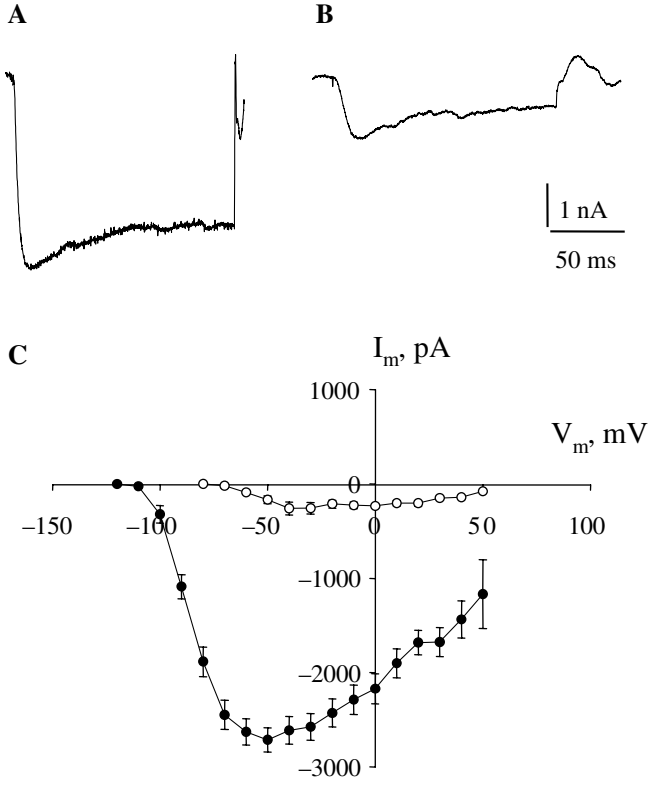

Fig. 2 Whole-cell currents recorded in pharyngeal muscle cells. **a**, **b** Examples of inward currents recorded from two different pharynxes at steps to −20 mV (**a**) and −50 mV (**b**) from a holding potential of −120 mV. The presence of notches on the current trace is indicative of incomplete space clamp. **c** Current–voltage plots for the peak inward current during steps from −120 mV (*black symbols*, averaged for 32 cells) and during steps from −80 mV (*open symbols*, $n = 4$). Internal solution contains NmDG in **a**–**c**

Previously, intracellular recordings from the pharynx have reported that the resting membrane potential of the terminal bulb in Dent's saline is relatively high, in the range of −65 to −80 mV (Pemberton et al. 2001; Franks et al. 2002). In whole-cell recording experiments, depolarising steps from holding potentials (V_h) in the range of the resting membrane potential i.e. from −80 mV, elicited small inward currents that peaked around −40 mV (Fig. 2c). In contrast, depolarising voltage steps from more negative holding potentials (−120 mV) routinely elicited inward currents of up to 3 nA. One possible explanation is that holding the membrane at a negative potential of −120 mV before the depolarising step may remove channel inactivation.

In order to test whether the inward current was carried by anions we made whole-cell recordings in low chloride external solution (70 mM NaCl replaced by 70 mM sodium isethionate). This would be predicted to shift the equilibrium potential for chloride ions and increase the amplitude of the inward current recorded following steps to −50 mV. However, the inward current was not significantly altered in low external chloride (−1,741 ± 281 pA in Dent's saline compared to −1,432 ± 123 pA in low chloride Dent's saline; $n = 4$; step from −120 to −50 mV) indicating that it is not carried by chloride ions. We also tested whether the voltage-activated inward current was sensitive to block by amiloride, as this is a blocker of T-type calcium currents (Tang et al. 1988). However, amiloride (100 μM) was without significant effect on the amplitude of the inward current (control current amplitude −2,724 ± 233 pA compared to −2,475 ± 219 pA, $n = 14$) and therefore the current does not exhibit this pharmacological property of conventional T-type calcium channels.

Effects of external calcium and sodium on voltage-activated inward currents

In order to determine the relative contribution of calcium and sodium to the voltage-activated inward currents, the effect of removing these ions from the external solution, and the effect of inorganic ion channel blockers, on the amplitude of currents was determined.

Removal of calcium from the external solution had no significant effect on the current amplitude ($n = 3$; Fig. 3a, d). As some current through calcium channels may be carried by magnesium ions, the effect of calcium-free magnesium-free solution was also tested. The amplitude of the peak current was slightly, but not

significantly, reduced in amplitude (−1,455 ± 321 pA, $n = 5$) compared to currents recorded in Dent's saline (−1,778 ± 370, $n = 5$; data not shown). In contrast, removal of external sodium, by replacement of external sodium with *N*-methyl-D-glucamine, in the presence of 3 mM calcium, reduced the amplitude of the short latency current recorded at steps to −50 mV ($n = 4$; $P < 0.01$, $n = 4$; Fig. 3b, d). We repeated these experiments in external solution from which both sodium and calcium had been removed. In these conditions, the inward current was also significantly reduced ($n = 4$; $P < 0.05$; Fig. 3c, d) although a small inward current still persisted. This was not tested further. Increasing the extracellular calcium concentration to 10 mM caused a slight, but insignificant increase of the currents ($n = 6$; Fig. 3d). These experiments suggest that in the absence of external calcium, sodium may act as the charge carrier. This is similar to observations reported for cardiac myocytes (Cole et al. 1997; Santana et al. 1998). However, these experiments also suggest that in *C. elegans* pharynx, in the absence of external sodium, calcium is less effective at carrying the inward current elicited by low threshold voltage activation.

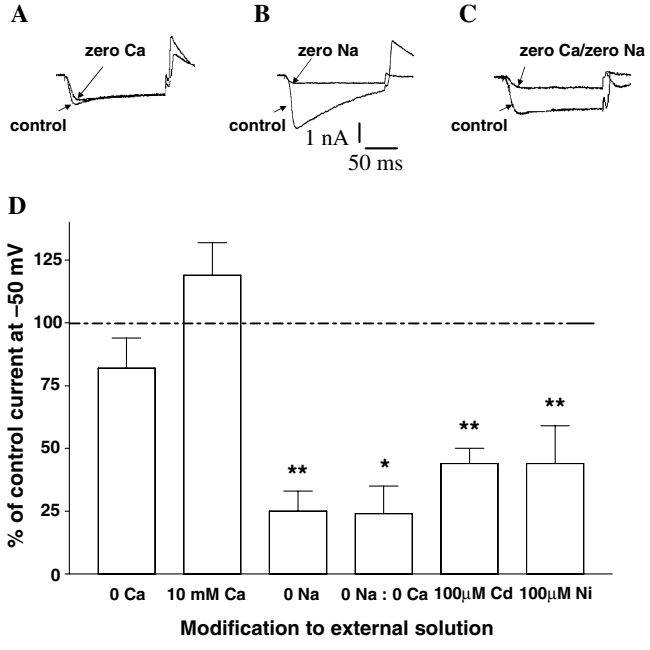

Fig. 3 The effect of the ionic composition of the external solution on the amplitude of the peak inward current. **a**–**c** Examples of the effects of ionic substitution on currents elicited by voltage steps from −120 to −60 mV (NmDG internal solution). Similar effects were observed at all voltage steps less than −120 to −50 mV. **d** A summary of the experiments investigating the effect of external ions on the amplitude of the peak inward current recorded at steps to −50 mV. The comparison between the amplitude of the current in Dent's saline (*control*) and in the different external (test) solutions (as shown on the *x axis*) has been made by expressing the amplitude of the current in the test solution as a percentage of the amplitude in the control solution for each pharyngeal recording. Data are the mean ± standard error of the mean. Statistical difference with respect to control was tested on the un-normalized data using the paired Student's *t* test. *$P < 0.05$; **$P < 0.01$

An L-type calcium channel reduction of function mutant, *egl-19* (*n582*), also exhibited voltage-activated inward currents at steps to −50 mV that were significantly and reversibly reduced in external solution containing zero sodium with 3 mM calcium (−3,592 ± 198 pA compared to −737 ± 296 pA in zero sodium, 3 mM calcium; $P < 0.001$, $n = 4$). An example is shown in Fig. 4a. As we were unable to accurately compensate for cell capacitance we were unable to make comparisons of current densities between the pharynxes of wild-type animals and *egl-19* mutants. However, the short-latency currents in *egl-19* were not obviously different from wild-type. A more recent detailed analysis has shown that in *egl-19* the activation time constant for the high voltage-activated inward current is increased (Shtonda and Avery 2005).

We had previously noted that veratridine, a toxin that selectively blocks voltage-gated sodium channel inactivation, induces repetitive firing of pharyngeal action potentials (Franks et al. 2002). In whole cell recordings we observed that veratridine (20 μM) increased the current amplitude but the effect was variable and not statistically significant (control −1,823 ± 418 pA compared to −2,027 ± 321 pA in 20 μM veratridine, $n = 5$; $P = 0.08$, Student's paired *t* test). However, current elicited in the presence of veratridine was markedly reduced in the absence of external sodium (control −2,058 ± 326 pA compared to 613 ± 281 pA in the

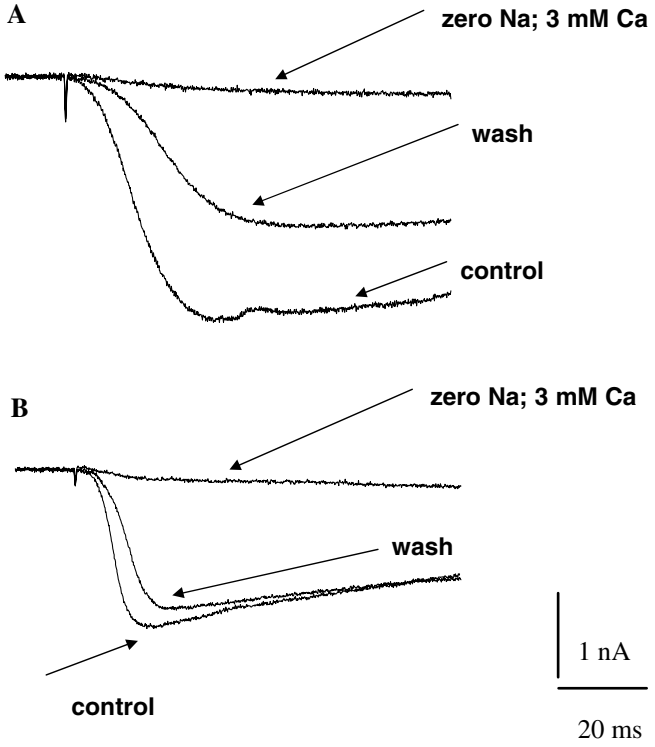

Fig. 4 **a** Currents recorded from the pharynx of an *egl-19* (*n582*) mutant (Cs internal solution). **b** Currents recorded from the pharynx of a wild-type animal that has been treated with veratridine (20 μM; NmDG internal solution) in Dent's solution (*control*), zero sodium external solution and the restoration of the current after returning to Dent's solution

absence of external sodium, $n = 5$, $P < 0.005$; Fig. 4b). The marked effect of removing external sodium on the currents recorded from pharynxes that had been treated with veratridine may be explained if this toxin increases the selectivity of the channel mediating the inward current for sodium ions.

Overall, these data show that the inward currents are significantly reduced in zero external sodium in three situations; in wild-type animals, in the presence of veratridine, and in *egl-19* animals.

Despite being more sensitive to changes in extracellular sodium than calcium, the voltage-activated inward currents were partially blocked by the divalent cations cadmium, nickel and barium (Figs. 3d, 5). Cadmium was effective at concentrations above 100 μM (Fig. 5a, d). At 1 mM cadmium, the current elicited by a voltage-step to −50 mV was reduced by 52 ± 8% ($n = 3$; $P = 0.002$). Nickel reduced inward currents only when used in concentrations as high as 1 mM by 49 ± 15% ($n = 5$; $P = 0.008$, Figs. 3d, 5). Unlike cadmium, the effect of 1 mM nickel was reversible (data not shown). Barium blocked the current at high concentrations only. Ten millimole barium caused an irreversible block of the current by 71 ± 2% ($n = 3$; $P = 0.03$).

Pharmacologically, the short latency low-threshold inward current in the pharyngeal muscle of *C. elegans* is unusual, as it combines a partial dependence on external sodium ions with sensitivity to inorganic calcium channel blockers.

Single-channel recordings in outside-out patches of pharyngeal muscle

Outside-out recordings were made with Dent's saline as the external solution, and caesium chloride internal solution i.e. the same ionic medium as used for whole cell recordings. Examples of the currents recorded at the different holding potentials are shown in Fig. 6a. In these conditions at a steady-state V_h of −80 mV channel currents showed a single, normal distribution (Fig. 6b) with a slope conductance of 19 pS and a reversal potential of +20 mV ($n = 22$; Fig. 6c). (The calculated reversal potential for sodium ions is +66 mV.) The reversal potential was not altered by the removal of intracellular chloride, i.e. using Cs-aspartate solution in the recording electrode ($n = 3$; Fig. 6c).

We tested whether the channels exhibited voltage-dependence. The latency to the first opening decreased immediately following a depolarising voltage step (223.9 ± 21.0 ms, $n = 14$, from −100 to −70 mV compared to 122.0 ± 11.20 ms, $n = 14$, $P < 0.002$, from −100 to 0 mV). However, there was no significant difference in open probability (data not shown; $n = 14$) and we were unable to reproduce the shape of the macroscopic current with ensemble averaging of 200 steps from −100 to −30 mV. The open-time distributions for the channels at −80 and +40 mV are shown in Fig. 6d. There was a shift to longer channel openings as described by the exponential for the distribution which had an increase in time-constant, tau (τ), at depolarised potentials (Fig. 6d). An example of the dependence of τ on the membrane holding potential is illustrated by Fig. 6e. From 20 outside-out patch recordings the mean τ at −80 mV was 0.49 ± 0.1 compared to 0.73 ± 0.1 ms at +40 mV (Student's paired t test, $P < 0.01$).

The single-channel conductance and reversal potential were not altered by the removal of extracellular calcium ($n = 4$; Fig. 7a, b). Nor did omission of potassium from the external solution significantly affect the characteristics of the current, although it was slightly increased in amplitude (−2.12 ± 0.15 pA compared to −2.36 ± 0.43 pA in zero external potassium; $n = 4$). However, the single-channel current amplitude at Vh −80 mV was reduced in the absence of external sodium (control −2.57 ± 0.15 pA compared to zero sodium −1.51 ± 0.26 pA; $n = 5$; $P < 0.02$; Fig. 8a, b). This reduction in the amplitude for single-channel currents in zero external sodium was observed for currents recorded at steady state but not when channels were recorded

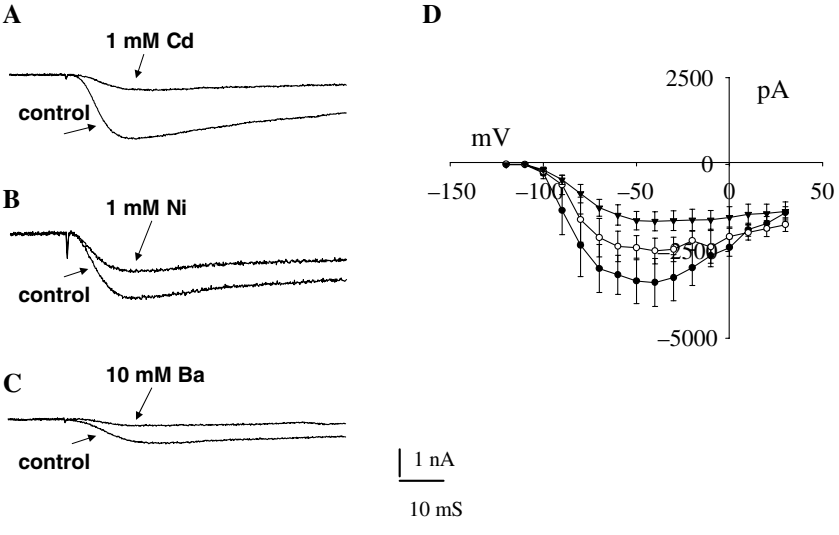

Fig. 5 The effects of the inorganic calcium channel blockers cadmium, nickel and barium on the amplitude of the peak inward current recorded at steps to −50 mV. **a** 1 mM cadmium (Cs internal solution). **b** 1 mM nickel (Cs internal solution) and **c** 10 mM barium (NmDG internal solutuion). **d** Current–voltage plots in Dent's solution (*control*; *black circles*), 0.1 mM cadmium (*open circles*) and 1 mM cadmium. $n = 3$; data are mean ± standard error of the mean

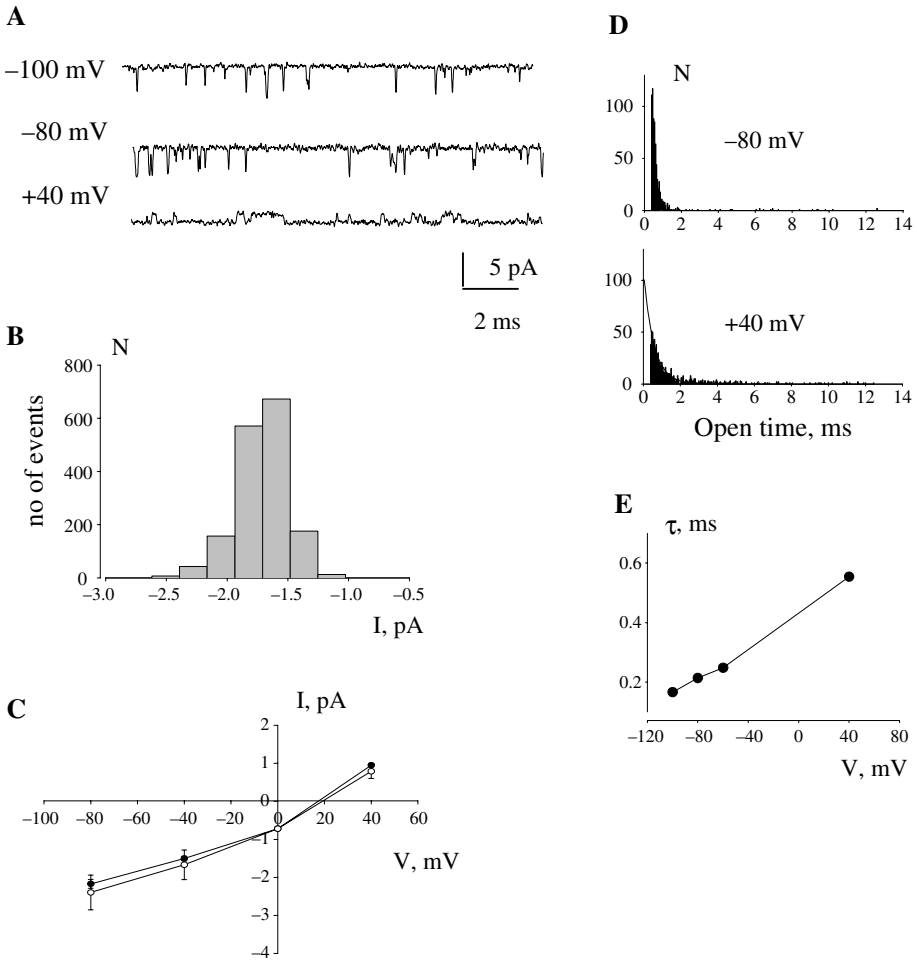

Fig. 6 Characteristics of single-channel currents recorded in an outside-out patch of pharyngeal muscle. **a** Examples of single-channel activity recorded in a patch at different holding potentials. **b** Amplitude distribution of the unitary currents in a patch held at −80 mV. **c** Current–voltage plots for single-channels recorded with either CsCl solution (*black circles*, $n = 18$) or Cs-aspartate (*open circles*, $n = 3$) as the internal solution. **d** Changes in the single-channel open-time distribution at the different holding potentials corresponding to the patch at **a**. Note the reduction of short opening events at +40 mV. **e** The voltage-dependence of the time constant of the open-time distributions corresponding to the patch shown in **a**

during instantaneous depolarising steps from −80 mV (Fig. 8c). To test whether sodium ions made any contribution to the single-channel currents recorded during instantaneous voltage-steps these experiments were repeated in low external sodium i.e. 14 mM, with 3 mM calcium. In these conditions, the single-channel current amplitudes during instantaneous depolarising steps were reduced and the reversal potential for the current was shifted to ∼0 mV (Fig. 8d). In zero sodium, zero calcium external solution the amplitudes of the single-channel currents was reduced, and completely blocked in four out of eight patches (Fig. 8e).

Single-channel activity in outside-out patches was sensitive to veratridine (20 μM; $n = 4$; Fig. 9a). Veratridine changed the open-time distribution of the channels at the holding potential of −80 mV and increased τ of the distribution (Fig. 9b). Channel activity observed during steps from V_h −100 to −30 mV increased after addition of 20 μM veratridine (Fig. 9c).

Single-channel recordings in inside-out patches of pharyngeal muscle

Sodium and calcium permeable channels could be recorded in inside-out patches of the pharyngeal muscle. In inside-out patches exposed to symmetrical 150 mM sodium solution, higher channel activity was observed ($n = 11$; Fig. 10a, two upper records; P_o at −80 mV 0.102 ± 0.017; chord conductance at −80 mV 35 ± 4.6 pS) than in symmetrical 5 mM calcium solution ($n = 20$; Fig. 10b; P_o at −80 mV 0.022 ± 0.005; chord conductance at −80 mV 17.4 ± 0.9 pS). When both sodium (150 mM) and calcium (3 mM) were present on the external face of the membrane, the unitary conductance of the currents was less than in symmetrical sodium ($n = 9$; Fig. 10a lower two traces; chord conductance at −80 mV 24.7 ± 3.1 pS; P_o 0.034 ± 0.024). These data are consistent with the proposal that calcium added to the sodium solution on the extracellular face of the membrane modulates channel conductance.

Discussion

The whole cell inward currents in the pharynx have different properties from other voltage-activated inward currents previously described in *C. elegans*. For example, calcium currents in neurones were increased in the presence of barium (Goodman et al. 1998) and calcium currents recorded from body wall muscle are abolished

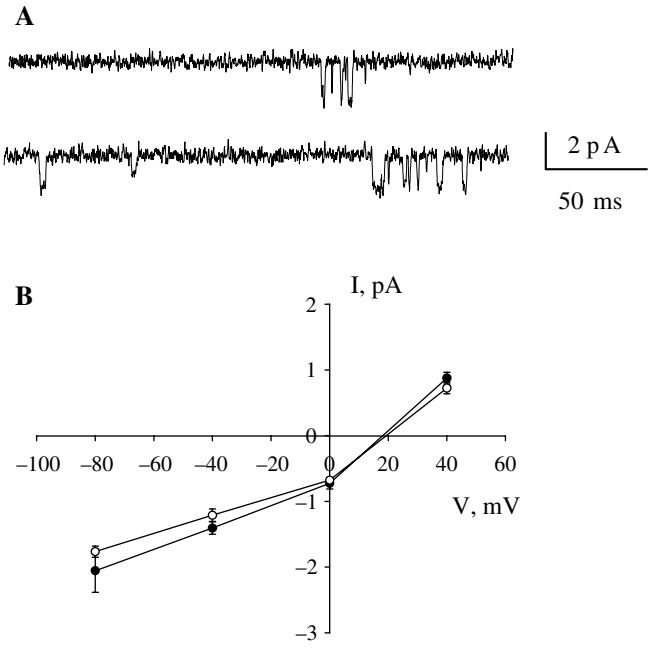

Fig. 7 Single-channel currents recorded in an outside-out patch in Dent's solution (**a**, *upper trace*) and in zero external calcium solution (**a**, *lower trace*). **b** The steady-state current–voltage plot in control (*black symbols*) and zero external calcium (*open symbols*). $n = 3$

in zero calcium and by cadmium (Richmond and Jorgensen 1999). In contrast, the voltage-activated inward currents in the pharynx, elicited by depolarisations from the holding potential to potentials up to −50 mV, were relatively unaffected by changes in external calcium ion concentration whereas removing external sodium ions reduced the current amplitude. This dependence on external sodium was also observed in a reduction of function mutant for an L-type calcium channel, *egl-19* (*n582*) and in the presence of the sodium channel toxin veratridine, which interacts selectively with voltage-activated sodium channels (Ohta et al. 1973). As might be expected, removal of both sodium and calcium ions from the external solution resulted in a very marked reduction in the amplitude of the inward current, although a small inward current still persisted. As potassium ions are present in the external but not the internal solution it is likely that this ion carries the residual current.

One channel that may contribute to the low voltage-activated inward current in the pharynx is CCA-1 (Shtonda and Avery 2005). This is a putative low voltage-activated T-type calcium channel subunit. The ionic permeability of this channel has not yet been described, and it could contribute to the currents that are described in this paper. If so, the low voltage-activated current does not exhibit some properties of conventional vertebrate T-type calcium currents. For example, it was not blocked by amiloride, nor was it depressed barium ions (Barrett et al. 2000). However, the inward current could be significantly reduced by the inorganic T-type calcium channel blocker, nickel, similar to the observation of Shtonda and Avery (2005) on the *cca-1* mediated low voltage-activated current in the pharynx. Cadmium also blocked the inward current. Although conventionally regarded as an inorganic calcium channel blocker, it is worthy of note that cadmium is also known to block TTX-resistant cardiac sodium channels in vertebrates (Backx et al. 1992). Furthermore, we cannot discount the possibility that the effects observed with the ion channel blockers are a consequence of a decrease in the coupling coefficient between the pharyngeal muscle cells.

Further evidence for a role for sodium ions in generating inward currents in the pharyngeal muscle was obtained from single-channel recordings in an outside-out patch configuration. This enabled channels in the same patch to be studied in external solutions with different ionic compositions for comparison with the results obtained from the whole cell recordings. In the first instance, the voltage-sensitivity of the channels in the patch recordings was determined. A number of approaches were used; ensemble averaging of 200 depolarising voltage steps, measurements of changes in open probability (P_o) with depolarisation, measurements of the first latency to channel opening following a depolarising step, and measurements of the open-time distribution (tau) at depolarised potentials. Of these, the latter two indicated that the channels are voltage-dependent. However, there was no significant increase in NP_o at depolarised potentials i.e. the effect of depolarisation is to elicit longer duration, but fewer, channel openings. We were also unable to reconstruct the shape of the macroscopic current by ensemble averaging of the single-channel events. Therefore the contribution of these single-channel currents to the whole-cell inward current is still not clear. Overall, the increase in the single-channel opening time, the increase in the value of tau for the open-time distribution curve in response to depolarisation and the decrease in the first latency of unitary currents during the depolarising steps are in favour of voltage-dependence of the channels, but the absence of a significant increase in NP_o during depolarising steps argues against it. One possible explanation for this discrepancy may be that gating properties of channels depend on their intact connection to the cytoskeleton (Chandler et al. 1976; Rios and Brum 1987; Shcherbatko et al. 1999) and may be modified in the process of excising patches.

A comparison of the unitary conductance of the single channels (19 pS) with those reported for other calcium channels indicate that it has a higher value compared to the conductance for T-type calcium channels (9 pS in 110 mM barium; Barrett et al. 2000) and L-type calcium channels in vertebrate cardiac muscle cells (6.9 pS in 10 mM calcium; Rose et al. 1992; 5 pS in 2 mM calcium; Guia et al. 2001). In contrast, voltage-gated sodium channels in mouse skeletal muscle have a conductance of 23.5 pS in physiological saline (Patlak 1988).

The ionic selectivity of the single channels was investigated by altering the ionic composition of the

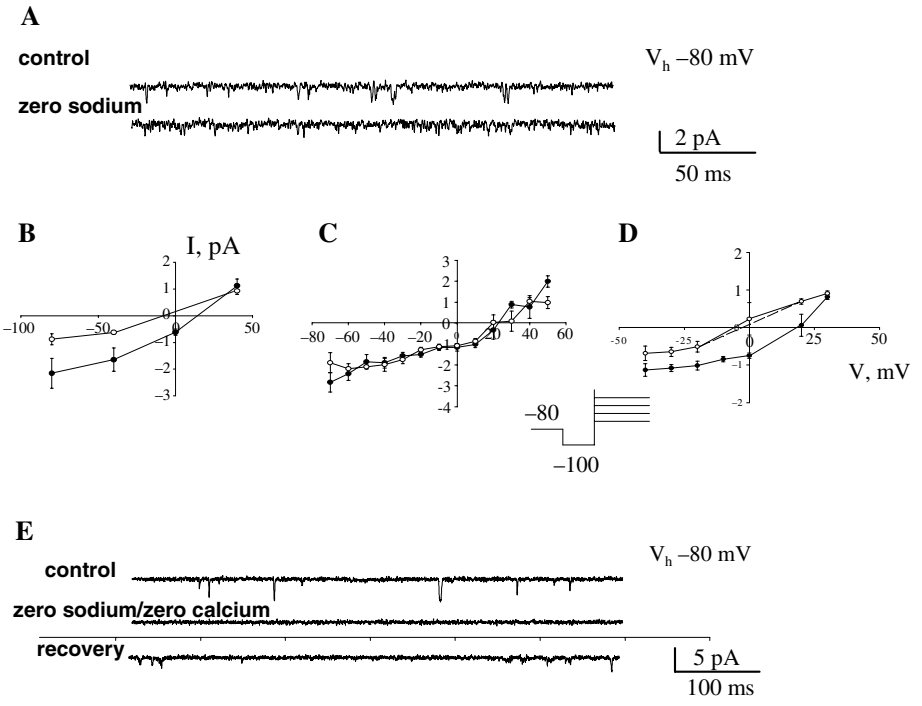

Fig. 8 The effect of external cations on single-channel currents recorded in outside-out patches. **a** Single-channel activity recorded in a patch (V_h −80 mV) in control Dent's solution (i.e. 140 mM sodium and 3 mM calcium; *upper trace*) and in the absence of external sodium (*lower trace*). **b** Reduction of the steady-state current amplitudes at negative potentials and shift in E_{rev} in patches exposed to Dent's solution (*black circles*) and after omission of sodium ions (*open circles*) in six outside-out patches. **c** Current–voltage relationship during 10 mV incremental steps from −80 mV (after a pre-pulse to −100 mV) in Dent's solution (*black circles*) and in zero external sodium solution (*open circles*; $n = 6$). **d** Current–voltage relationship obtained for eight outside-out patches during 10 mV incremental steps from −80 mV (after a pre-pulse to −100 mV) in Dent's solution (*black circles*) and 14 mM sodium, zero calcium solution (*open circles*). **e** Consecutive recordings of single-channel activity in an outside-out patch. The *top trace* shows single-channel recordings in Dent's solution, the *middle trace* in zero external sodium, zero external calcium solution and the *bottom trace* in Dent's solution again

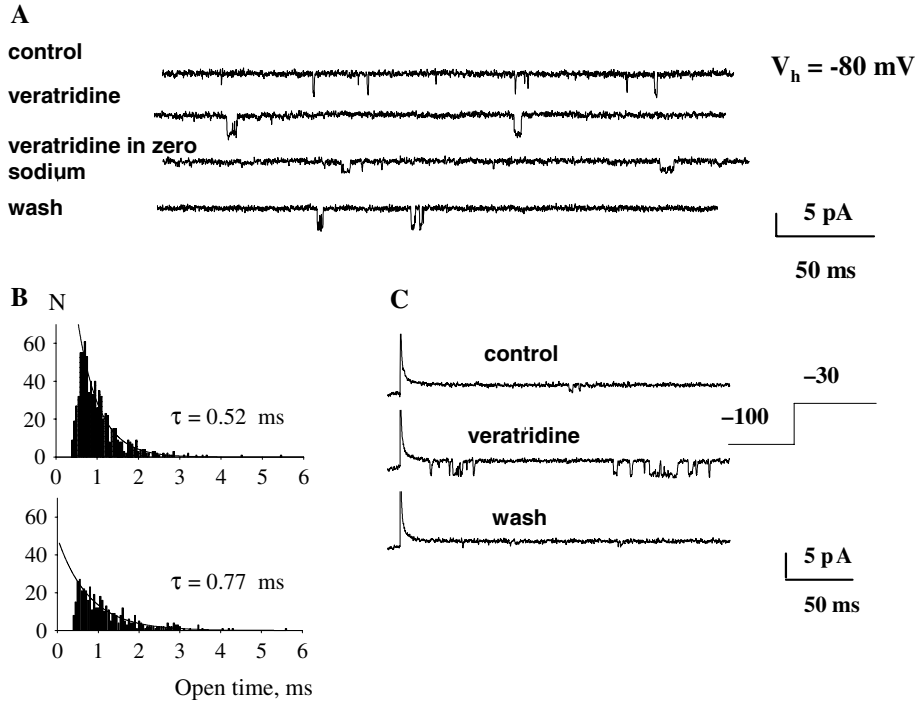

Fig. 9 The effect of veratridine on single-channel activity. **a** Single-channel recording from an outside-out patch. The traces are (from the *top down*): control recording (in Dent's solution); with 20 μM veratridine; zero sodium and 3 mM calcium with 20 μM veratridine; and wash to Dent's solution. **b** Open-time distribution for single channels in an outside-out patch in Dent's solution (*upper plot*, $\tau = 0.52$ ms) and after application of 20 μM veratridine ($\tau = 0.77$ ms). V_h −80 mV. **c** Increased single-channel activity during steps from V_h −100 to −30 mV in the presence of 20 μM veratrdine (*middle trace*). *Upper and lower traces* correspondingly before and after veratridine application

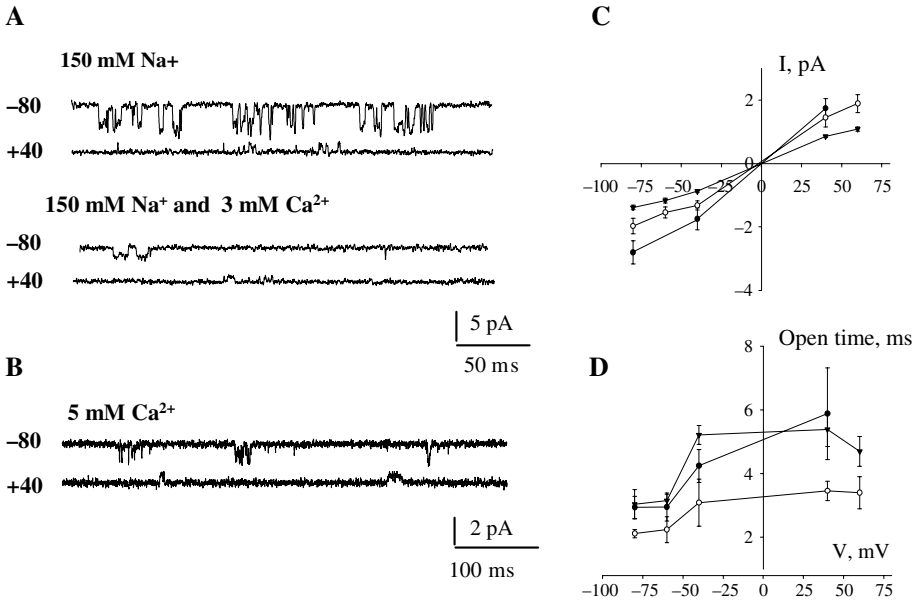

Fig. 10 Single-channels currents recorded in inside-out patches. **a** The top pair of records show examples of currents recorded in 150 mM sodium zero calcium symmetrical solution at −80 and +40 mV. The lower pair of records shows the currents recorded when 3 mM calcium was included in the pipette solution, i.e. on the extracellular side of the membrane. **b** Examples of currents recorded from a patch in 5 mM calcium zero sodium symmetrical solution at −80 and +40 mV. (Note the difference in amplification.) **c** A comparison of I–V curves in inside-out patches in 150 mM sodium zero calcium symmetrical solution (*filled circles*, $n = 11$), in 150 mM sodium with 3 mM calcium added to the solution on the external side of the membrane (*open circles*, $n = 9$), and in 5 mM calcium zero sodium symmetrical solution (*black triangles*, $n = 20$). **d** The increase in the open time of channels with depolarisation steps from −80 mV with a pre-pulse to −100 mV. Symbols are the same as on **c**

external solution. Removing calcium ions had little effect on the amplitude of single-channel currents recorded at steady-state whereas removing sodium ions decreased the amplitude of the channels indicating the channel may be selective for this cation. However, the interpretation of this was complicated by observations made on the ionic dependence of single-channels recorded following instantaneous voltage-steps. The amplitude of these channels was not reduced in zero sodium with 3 mM calcium ions, although in low external sodium with zero calcium there was a shift in the reversal potential, consistent with a role for sodium as a charge carrier. However, this shift was 20 mV, less than that predicted by the Nernst equation. A possible explanation for this is that the channels are permeant to caesium ions which are present in the internal solution. In this context it is interesting to note that the results from the whole-cell recordings indicated that in the absence of sodium and calcium ions that the current may be carried by potassium, and furthermore that there are examples of the permeability of calcium channels to caesium (e.g. Dirksen and Beam 1999).

Inward currents were also recorded in inside-out patches in symmetrical ionic solution. These channels had a similar unitary conductance to those recorded in outside-out patches under comparable conditions. They also exhibited an increase in open-time at depolarised potentials. A comparison was made between the single-channel currents in the presence of sodium ions alone, calcium alone, or in symmetrical sodium with calcium on the external face of the membrane. This latter experiment showed that the presence of calcium did not shift the reversal potential, but did reduce the unitary conductance of the channels. This observation is consistent with the proposal that the channels conduct sodium in preference to calcium. However, a limitation of this study is that it has not yet been possible to make a direct comparison of the single-channel conductance before and after addition of calcium ions to the external face of the membrane in symmetrical sodium solution.

The properties of the channels that contribute to the pharyngeal muscle inward currents require further characterization. An intriguing possibility, still not resolved, is that there may be a voltage-gated channel which combines a preference for sodium ions over calcium and veratridine sensitivity, with sensitivity to inorganic calcium channel blockers. There is a close structural relationship between voltage-gated sodium and calcium channels and relatively small changes in the amino acid sequence of the pore region can confer selectivity of the channel for one cation over the other. It has been shown that replacing glutamate residues in the SS2 segments alters the ion selectivity of the cardiac calcium channels, making them more permeable to sodium (Tang et al. 1993) or lithium (Yang et al. 1993) than to calcium, while two single mutations of the rat sodium channel II switch its selectivity from sodium to calcium (Heinemann et al. 1992). The high permeability of calcium channels for sodium ions has long been appreciated (Kostyuk et al. 1983; Almers and McClesky

1984; Hess and Tsien 1984), but has been confined to the measurement of currents in calcium-free solutions, as in the presence of calcium, the conductance of sodium ions is blocked (Carbon et al. 1997). It should also be mentioned in this connection that a prokaryote sodium channel with pharmacological properties resembling a calcium channel has been described (Ren et al. 2001).

In summary, the ion replacement experiments described here have provided evidence for inward currents operating in the pharyngeal muscle of *C. elegans* that are reduced in amplitude when sodium ions are removed from the external solution. This, combined with the observation that veratridine and procaine can affect the activity of pharyngeal muscle (Franks et al. 2002), lends further support to the idea that a channel with at least some properties in common with vertebrate voltage-gated sodium channels may be present in *C. elegans*.

Acknowledgements This project was funded by the Biological and Biotechnology Research Council, UK. We gratefully acknowledge the *C. elegans* Genetics Centre, which is funded by the NIH National Center for Resources, for provision of some strains. We are also grateful to Dr P. Bregestovski (INMED, Marseille) for valuable advice on single-channels recording.

References

Almers W, McClesky EW (1984) Non-selective conductance in calcium channels of frog muscle: calcium selectivity in a single-file pore. J Physiol 353:585–608

Avery L, Horvitz R (1989) Pharyngeal pumping continues after laser killing of the pharyngeal nervous-system of *C. elegans*. Neuron 3:473–485

Backx PH, Yue DT, Lawrence JH, Marban E, Tomaselli GF (1992) Molecular localization of an ion-binding site within the pore of mammalian sodium channels. Science 257:248–251

Bargmann CI (1998) Neurobiology of the *Caenorhabditis elegans* genome. Science 282:2028–2033

Barnes S, Hille B (1988) Veratridine modifies open sodium channels. J Gen Physiol 91:421–443

Barrett PQ, Lu HK, Colbran R, Czernik A, Pancrazio JJ (2000) Stimulation of unitary T-type Ca^{2+} channel currents by calmodulin-dependent protein kinase II. Am J Physiol Cell Physiol 279:C1694–C1703

Carbon E, Lux HD, Carabelli V, Aicardi G, Zucker H (1997) Ca^{2+} and Na^{+} permeability of high-threshold Ca^{2+} channels and their voltage-dependent block by Mg^{2+} ions in chick sensory neurones. J Physiol 504:1–15

Chandler WK, Rakowski RF, Schneider MF (1976) Effects of glycerol treatment and maintained depolarisation on charge movement in skeletal muscle. J Physiol 254:285–316

Cole W, Chartier D, Martin M, Lebranc N (1997) Ca^{2+} permeation through Na^{+} channels in guinea-pig ventricular myocytes. Am J Physiol 273:H129–H137

Dirksen RT, Beam KG (1999) Role of calcium permeation in dihydropyridine receptor function. Insight into channel gating and excitation-contraction coupling. J Gen Physiol 114:393–403

Franks CJ, Pemberton D, Vinogradova I, Cook A, Walker RJ, Holden-Dye L (2002) The ionic basis of the resting membrane potential and action potential in the pharyngeal muscle of *Caenorhabditis elegans*. J Neurophysiol 87:954–961

Goodman MB, Hall DH, Avery L, Lockery SR (1998) Active currents regulate sensitivity and dynamic range in *C. elegans* neurones. Neuron 20:763–772

Guia A, Stern MD, Lakatta EG, Josephson IR (2001) Ion concentration-dependence of rat cardiac unitary L-type calcium channel conductance. Biophys J 80:2742–2750

Hart AC, Sims S, Kaplan JM (1995) Synaptic code for sensory modalities revealed by *C. elegans* glutamate receptor. Nature 378:82–85

Heinemann SH, Terlau H, Stühmer W, Imoto K, Numa S (1992) Calcium channel; characteristics conferred on the sodium channel by single mutations. Nature 356:441–443

Hess P, Tsien RW (1984) Mechanism of ion permeation through calcium channels. Nature 309:453–456

Horn R, Vandenberg CA (1984) Statistical properties of single sodium channels. J Gen Physiol 84:505–534

Jorgensen EM, Nonet ML (1995) Neuromuscular junctions in the nematode *C. elegans*. Dev Biol 6:207–220

Jospin M, Jacquemond V, Mariol MC, Segalat L, Allard B (2002) The L-type voltage-dependent Ca^{2+} channel EGL-19 controls body wall muscle function in *Caenorhabditis elegans*. J Cell Biol 159:337–348

Kostyuk PG, Mironov SL, Shuba YM (1983) Two ion-selecting filters in the calcium channel of the somatic membrane of mollusc neurones. J Membr Biol 76:83–93

Lee RYN, Lobel L, Hengartner M, Horvitz HR, Avery L (1997) Mutations in the α1subunit of an L-type voltage-activated Ca^{2+} channel cause myotonia in *Caenorhabditis elegans*. EMBO J 16:6066–6076

Li H, Avery L, Denks W, Hess GP (1997) Identification of chemical synapses in the pharynx of *Caenorhabditis elegans*. Proc Natl Acad Sci USA 94:5912–5916

Maricq AV, Peckol E, Driscoll M, Bargmann CI (1995) Mechanosensory singalling in *C. elegans* mediated by the GLR-1 glutamate receptor. Nature 378:78–81

McKay JP, Raizen DM, Gottschalk A, Schafer WR, Avery L (2004) EAT-2 and EAT-18 are required for nicotinic neurotransmission in *Caenorhabditis elegans* pharynx. Genetics 166:162–169

O'Hagan R, Chalfie M, Goodman MB (2005) The MEC-4/DEG/ENaC channels of *Caenorhabditis elegans* touch receptor neurones transduces mechanical signals. Nat Neurosci 8:7–8

Ohta M, Narahashi T, Keeler RF (1973) Effects of veratrum alkaloids on membrane potential and conductance of squid and crayfish giant axons. J Pharmacol Exp Ther 184:143–154

Patlak JB (1988) Sodium channel subconductance levels measured with a new variance-mean. J Gen Physiol 92:413–430

Pemberton DJ, Franks CJ, Walker RJ, Holden-Dye L (2001) Characterisation of a glutamate-gated chloride channels in the pharynx of wild-type and mutant *Caenorhabditis elegans* delineates the role of the subunit GluCl-α2 in the function of the native receptor. Mol Pharmacol 59:1037–1043

Raizen DM, Lee RYN, Avery L (1995) Interacting genes are required for pharyngeal excitation to motorneurone MC in *Caenorhabditis elegans*. Genetics 141:1365–1382

Ren D, Navarro B, Xu H, Yue L, Shi Q, Clapham DR (2001) A prokaryotic voltage-gated sodium channel. Science 294:2372–2375

Richmond JE, Jorgensen EM (1999) One GABA and two acetylcholine receptors function at the *C. elegans* neuromuscular junction. Nat Neurosci 2:791–797

Ríos E, Brum G (1987) Involvement of dihydropyridine receptors in excitation–contraction coupling in skeletal muscle. Nature 325:717–720

Rose WC, Balke CW, Wier WG, Marban E (1992) Macroscopic and unitary properties of physiological ion flux through L-type Ca2+ channels in guinea-pig heart cells. J Physiol 456:267–284

Santana LF, Gomez AM, Lederer WJ (1998) Ca^{2+} flux through promiscuous cardiac Na^{+} channels: slip-mode conductance. Science 279:1027–1033

Scherbatko A, Ono F, Mandel G, Brehm P (1999) Voltage-dependent sodium channel function is regulated through membrane mechanics. Biophys J 77:1945–1959

Shtonda B, Avery L (2005) CCA-1, EGL-19 and EXP-3 currents shape the action potential in the *Caenorhabditis elegans* pharynx. J Exp Biol 208:2177–2190

Starich TA, Lee RYN, Panzarella C, Avery L, Shaw JE (1996) *eat-5* and *unc-7* represent a multigene family in *Caenorhabditis elegans* involved in cell–cell coupling. J Cell Biol 134:537–548

Tang CM, Presser F, Morad M (1988) Amiloride selectively blocks the low threshold (T) calcium channel. Science 240:213–215

Tang S, Mikala G, Bahinski A, Yatani A, Varadi G, Schwartz A (1993) Molecular localization of ion selectivity sites within pore of a human L-type cardiac calcium channel. J Biol Chem 268:13026–13029

Ulbricht W (1969) The effect of veratridine on excitable membranes of nerve and muscle. Ergeb Physiol Biol Chem Exp Pharmacol 61:17–71

Wei A, Jegla T, Salkoff L (1996) Eight potassium channel families revealed by the *C. elegans* genome project. Neuropharmacology 35:805–829

Yang J, Ellinor PT, Sather WA, Zhang J-F, Tsien RW (1993) Molecular determinants of Ca^{2+} selectivity and ion permeation in L-type Ca^{2+} channels. Nature 366:158–161